Coherent Amplification of Ultrafast Molecular Dynamics in an Optical Oscillator

Igal Aharonovich* and Avi Pe'er†
Department of Physics and BINA Center for Nanotechnology, Bar-Ilan University, Ramat Gan 52900, Israel
(Received 20 March 2015; revised manuscript received 20 January 2016; published 18 February 2016)

Optical oscillators present a powerful optimization mechanism. The inherent competition for the gain resources between possible modes of oscillation entails the prevalence of the most efficient single mode. We harness this "ultrafast" coherent feedback to optimize an optical field in time, and show that, when an optical oscillator based on a molecular gain medium is synchronously pumped by ultrashort pulses, a temporally coherent multimode field can develop that optimally dumps a general, dynamically evolving vibrational wave packet, into a single vibrational target state. Measuring the emitted field opens a new window to visualization and control of fast molecular dynamics. The realization of such a coherent oscillator with hot alkali dimers appears within experimental reach.

DOI: 10.1103/PhysRevLett.116.073603

Compared to atoms, molecules are unique in their vibration and rotation, which produces rich, complex dynamics upon excitation by pulses of light [1]. Since chemical reactions are driven by vibrational dynamics [2], precise measurement and control of the vibration is of interest. To date, vibrational dynamics was measured using either pump-probe excitation or wave-packet tomography. In pump-probe excitation, a pump pulse excites the dynamics and a delayed probe pulse probes it, usually by selective ionization or dissociation of the molecule depending on its vibrational configuration [3–5]. In wave-packet tomography, the spontaneous emission from an excited vibrational wave packet is time-resolved, reflecting the vibration dynamics due to the time-dependent Franck-Condon overlap between the wave packet and the final state [6–9]. Both methods are inherently limited by the weak measured signal (less than one photon or electron per molecule per pump pulse), which is difficult to detect, indicating that both methods are inherently slow and require averaging (either in space over a large ensemble of molecules or in time over many pump pulses) to obtain a decent signal-to-noise ratio. While averaging incoherently accumulates the light intensity from many molecules, we present a method for coherent accumulation of the field amplitude in time that can dramatically improve the signal-to-noise ratio and speed of the measurement.

We suggest an optical oscillator, where coherent emission from a dynamically evolving wave packet (excited by an ultrashort pump pulse) is amplified beyond the oscillation threshold. The oscillator concept is outlined in Fig. 1: A medium of molecules is placed in an optical cavity and excited by ultrashort pump pulses with a repetition rate that matches the cavity round trip. Each pump pulse excites a nonstationary vibrational wave packet, which later coherently evolves (vibrates) on the excited electronic potential. During vibration, the wave packet emits nonstationary Raman light, either spontaneous or stimulated, as illustrated in Fig. 2, for a medium of K_2 molecules. In wave-packet tomography, this spontaneous Raman emission was temporally resolved to reconstruct the wave-packet dynamics [3,6,10]. We suggest collecting the emitted Raman light in a cavity, where stimulated amplification can occur when the pump repetition matches the cavity round trip, which ensures that the emission from one pump pulse returns to the medium synchronously with the next pulse. When such a Raman amplifier crosses threshold, a temporally coherent oscillation can be obtained, where the pump field that was inscribed onto the excited wave packet, is later reshaped by the vibrational dynamics and reemitted in the form of coherent Raman radiation. For simplicity, we assume that the pulse repetition is low compared to the decay rate of the molecules, indicating that the time between pulses is sufficiently long for all molecules to decay back to the ground vibrational level. Therefore, the molecules carry no memory of previous excitations, but the light field accumulated in the cavity serves as coherent memory that lingers from pulse to pulse.

Our method is related to work on precision control of molecular dynamics using the frequency comb [11–13], where highly efficient and selective population transfer was achieved between designated vibrational levels, relying on coherent accumulation of molecular excitations from a train of weak pump-dump pulse pairs, and a vibrational wave packet as an intermediate. The noticeable difference is that now the coherent memory is not in the molecules, but in the accumulated dump field, and the field is not prespecified, but rather amplified from spontaneous emission. Yet, the logic of coherent accumulation is identical, leading to selective transfer, and the theoretical treatment is similar, both for analytic calculation and numerical simulation of the dynamics.

Note the difference between the proposed coherent Raman oscillator and methods of coherent Raman spectroscopy [14,15], such as Raman fluorescence, stimulated Raman spectroscopy [16,17], and coherent anti-Stokes Raman

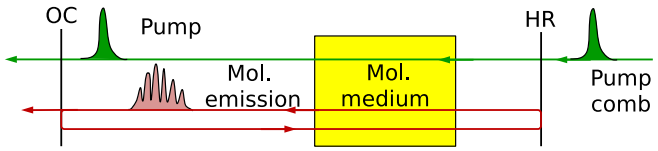

FIG. 1. Oscillator concept. A molecular medium in an optical cavity is excited by a train of pump pulses. Each pump pulse launches a vibrational wave packet, which later emits (Raman) light, as it vibrates on the excited molecular potential. The cavity, which resonates only the Raman emission (not the pump), is matched to the repetition rate of the pump pulses, allowing amplification of the Raman emission.

spectroscopy [18–20]. All these methods measure molecular vibrational levels in the ground electronic potential, and deliberately avoid the excited potential to ensure a purely virtual Raman transition between ground levels. In contrast, we aim to observe the vibrational dynamics in the excited electronic potential, and the pump pulses are tuned to excite a meaningful wave packet. In addition, the dump pulse is not externally set but, rather, amplified from spontaneous emission through coherent accumulation and is subject to mode competition.

In the analytic and numerical study presented here, we consider a realistic test case of a coherent Raman oscillator. As gain medium, we take an ensemble of alkali dimers (K_2 or Li_2) that are thermally mixed with free atoms in a hot vapor cell (~550° K for K_2, and ~700° K for Li_2) and show that the oscillation threshold is achievable with reasonable pump power (~1 W), molecular densities (10^{13-14} cm^{-3} for K_2) and interaction length (5–10 cm). We present the calculation and simulation in a bottom-up structure, from the microscopic, single molecule dynamics to the

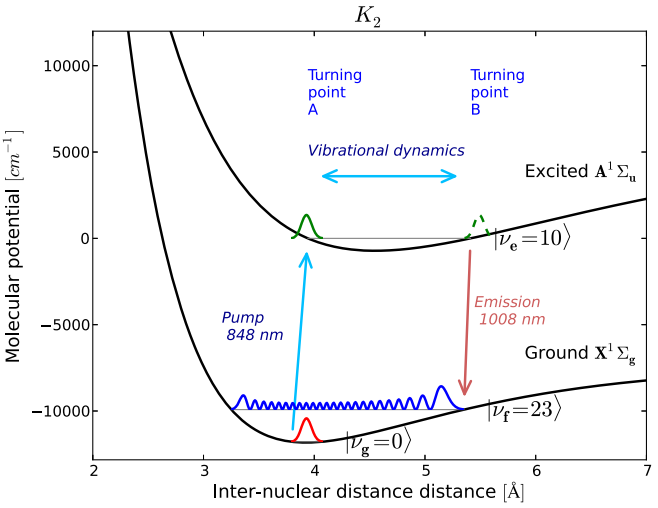

FIG. 2. Molecular excitation cycle for the K_2 dimer. The pump pulse excites a vibrational wave packet. As the wave packet vibrates and disperses on the excited potential, emission occurs primarily when the wave packet passes at the outer turning point B, where the Franck-Condon overlap is maximal to the target state (near vibrational level $\nu_f = 23$).

macroscopic field gain and cavity evolution, accounting for loss, dispersion, and decoherence. Since the performance of this coherent oscillator and, in particular, the oscillation threshold critically depend on decoherence properties, an in-depth evaluation of decoherence mechanisms is provided—both homogeneous pressure broadening (collisions) and inhomogeneous rotational and Doppler broadenings. We show that the homogeneous coherence time in a hot vapor cell can reasonably be $T_2 \geq 100$ ps, and that the threshold is primarily affected by the inhomogeneous thermal distribution of rotational states, which breaks the molecular ensemble into independent coherent clusters and reduces the available population for coherent gain. This Letter outlines the calculation concept, simulation procedure and results, and the decoherence considerations (with full details provided in the Supplemental Material [21]).

Before delving into the calculation, it is illuminating to present the unique features of this oscillator as reflected in the simulation results. Once Raman oscillation is obtained, this oscillator demonstrates unique coherent dynamics: The produced "dump" field, that stimulates the molecules back to the ground potential, forms, together with the pump pulse, a coherent pump-dump pair, reminiscent of many configurations of coherent control [33,34]. Here, however, the dump field is not specified *a priori* but is dynamically amplified from spontaneous emission. Therefore, the final target state of the molecules is also undefined, and different possible decay channels may compete for the gain (pump energy). Surprisingly, the winning decay channel near threshold is to dump the entire wave packet to a single target vibrational state with a train of dump pulses that is matched to the vibrational period of the excited wave packet (see Fig. 3). Furthermore, the quantum efficiency of the dump transfer is always near unity with very high target selectivity, even very close to threshold.

The oscillator harnesses mode competition to "automatically" solve an important optimization problem of coherent quantum control: to find the optimal dump pulse for efficient and selective transfer from a given wave packet to a single target state [11,12,35]. This automatic solution for the pulse in time is in direct analogy to work in [36], where the competition between spatial modes was exploited to generate the optimal field in space to focus through a highly scattering, turbulent medium. Single vibrational mode selection was also observed in a theoretical study of a proposed x-ray laser with a gain medium of N_2 molecules [37,38].

Although the final state is not designated *a priori* and is selected via intracavity mode competition, the dynamics can be steered towards a desired vibrational target state n_f by shaping the spectrum of the pump pulse to maximize the spectral overlap of the excited wave packet with the target state [11]. As detailed in the Supplemental Material [21], this is accomplished by enhancing (diminishing) pump frequencies that excite components of the wave packet with high (low) Franck-Condon overlap to the target state n_f. Specifically, shaping the pump spectrum according to

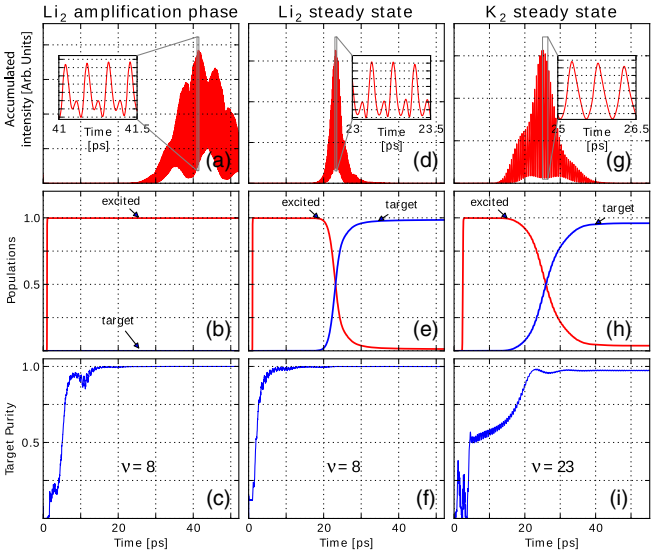

FIG. 3. Simulation results (for a single coherent cluster) for Li_2 and K_2 during 50 ps following a particular pump pulse excitation, for an oscillator pumped slightly above threshold. The left column shows the intracavity field and populations at an early stage of the amplification, well before saturation is reached (Li_2); the middle (Li_2) and right (K_2) columns show the results for stable oscillation. The top row shows the temporal intensity of the intracavity field, where the rapid oscillations (see inset) match with the vibrational dynamics of the excited wave packet. The middle row shows the corresponding evolution of the populations of the excited (red) and target (blue) wave packets. In the bottom row, the overlap of the target state with the designated target state is shown, demonstrating the high selectivity of the dump transfer.

$E_{\mathrm{pump}}(\omega_{n_e}) \propto \mu_{eg}\langle n_e|n_f\rangle$, where ω_{n_e} denotes the transition frequency from the initial ground state $n_g = 0$ to the vibrational component n_e of the excited wave packet. We verified this selective steering in simulation with Li_2, where shaping the spectrum of a given pump pulse steered the dump into any of the target states $n_f = 8, 9, 10$.

One can consider the emission from the coherent Raman oscillator as a Raman shifted version of optical free induction decay (FID), where a large ensemble of molecular dipoles emit coherently. Observation of FID in the optical domain is challenging since the emission is very short in time (limited by the coherence time T_2), and overlaps spectrally with the excitation pulse. Previously, optical FID was measured indirectly by Fourier inversion of the molecular absorption spectral amplitude (including phase), as measured with a dual frequency comb [39,40]. The large Raman shift in our oscillator allows optical FID to be observed directly in time. Furthermore, the excited wave-packet dynamics can be directly read off from the spectrum and phase of the emitted field, as elaborated in the Supplemental Material [21].

To model the coherent Raman oscillator we take an iterative approach, which mimics the intracavity evolution in time: the molecular radiated field in every round trip is calculated based on the, so far, accumulated intracavity field and on the recurring pump pulse excitation, both interacting coherently with the molecular ensemble. The cavity field for the next round trip is then generated by adding the emission to the previous intracavity field, including decoherence, cavity loss and dispersion. The emitted field E_{em} is proportional within the dipole approximation to the second time derivative of the total (macroscopic) electric dipole in the medium P_M

$$E_{\mathrm{em}}(z,t) = \frac{1}{4\pi z\varepsilon_0 c^2}\frac{d^2}{dt^2}P_M(t - z/c). \tag{1}$$

In a large ensemble, the total dipole is $P_M(t) = \mathcal{N}P(t)$, where $\mathcal{N}$ is the effective number of molecules and P is the quantum average dipole of a single molecule

$$P(t) = e^{-i\omega t}\mu_{eg}\langle\psi_g(t)|\psi_e(t)\rangle + \mathrm{c.c.} \equiv p(t)e^{-i\omega t} + \mathrm{c.c.} \tag{2}$$

Here, $|\psi_{g,e}(t)\rangle$ are the vibrational wave functions on the ground and excited electronic potentials, ω is the center optical frequency and $\mu_{eg} = \bar{\mu}_{ge} \equiv \mu$ is the electronic dipole moment between the potentials, assumed independent of the internuclear distance (Condon approximation). Thus, once the molecular wave-packet dynamics is calculated, the microscopic molecular dipole (and emitted field) can be easily obtained as the time dependent overlap between the excited and target wave packets (and its temporal derivatives).

Thus, the gain is calculated in three stages: First, given the pump pulse field, and the current cavity-accumulated dump field, the dynamics of the wave packet is calculated on all the coupled ground-excited-target potentials by numerically solving the time-dependent Schrödinger equation (using the split-operator method [41]). Once the wave functions are calculated in time, the average dipole and the emitted field (per molecule) are calculated with Eqs. (1) and (2). Last, the macroscopic field gain is calculated by considering the spatial mode of the emitted field and the total number of excited molecules. Cavity losses and dispersion are applied after every iteration, and spontaneous emission is modeled as an additive white noise to the emitted field, which seeds the oscillation. Homogeneous decoherence (collisional pressure broadening) is introduced as a phenomenological decay of the macroscopic dipole, whereas inhomogeneous decoherence is incorporated as an effective reduction of the available molecular population due to the thermal spread of rotations (J states), which divides the molecular population to independent coherent clusters of slightly shifted emission frequencies (see further details later on and a complete discussion in the Supplemental Material [21]).

The evolution of the Raman oscillator can then be simulated including all experimental parameters, the mode competition during cavity buildup can be fully visualized for both the wave-packet dynamics and the cavity field, and the emitted field in stable operation can be calculated. We simulated the coherent Raman oscillator for molecular media of alkali dimers Li_2, K_2, and Rb_2, using electronic Morse potential fits [42–44] for the ground $X^1\Sigma_g$ and excited $A^1\Sigma_u$ states. Transition dipole moments were assumed to be the spherically averaged atomic values of the D line [45].

Figure 3 shows snapshots of the accumulated field, the molecular populations and the vibrational selectivity for Li_2 and K_2 dimers for various stages of oscillator evolution (with a single oscillating coherent cluster). The results reveal exceptional features of this coherent Raman oscillator: (a) Complete dumping is obtained of the excited wave packet to the target state, even though the oscillator is pumped just a few percent above threshold. This is in contrast to standard lasers, where the excited state population clamps to the threshold value, and can never be completely dumped. (b) Near threshold, the emitted field forms a long train of pulses matched to the excited wave-packet vibration (see insets in the top row of Fig. 3). Note that the main emission develops only ~30 ps after the pump in spite of the shorter $T_2 = 25$ ps that was assumed. (c) The vibrational selectivity of the target state is exceptional near threshold. For Li_2, practically all the dumped population occupies a single vibrational state ($> 99.99\%$), and this selectivity is achieved rather early in time, even before the main bulk of the population is actually transferred. For K_2, selectivity is a little lower at $> 98\%$, and for Rb_2, the selectivity was $> 90\%$. These high selectivity values are achieved autonomously by the system due to the physical preference in the mode competition stage. This preference is directly related to the ratio of the excited vibrational period to the available coherence time T_2, which is best for the light and fast Li_2. (d) As the pump is increased further above threshold, the emitted pulse train becomes shorter and appears at an earlier time after the pump. The selectivity of the target state in K_2 is also gradually degraded, showing mixture of states (see Supplemental Material [21]). Li_2 shows a similar trend, but its selectivity is much more robust and is degraded only at much higher, rather impractical pump levels. (e) Conversely, as the pump is reduced towards threshold, the main oscillation is pushed towards longer times, until eventually suppressed by the decoherence window, and can no longer dump all the excited population to the target state. The threshold oscillation is, therefore, a direct result of the available coherence time, and if longer coherence is assumed, the threshold would be reduced, as, indeed, observed in our simulations.

To explain the above properties, we consider that, just like any laser, the coherent Raman oscillator "seeks" the most efficient channel to dump the excited population. Because of the coherent pumping, the oscillator can exploit coherent population transfer which the standard laser cannot (e.g., a π pulse). Specifically, by extending the coherent transfer over a longer time, a complete dump transfer can be achieved with a lower overall dump energy, just like in a simple two-level system, where the energy required for a π pulse is inversely proportional to its duration. Thus, near threshold, where the available energy for the dump is low, a long coherent train (limited by decoherence) develops. As the pump is increased above threshold, the available dump energy increases, and the population can be dumped faster.

The molecular dynamics, however, is far richer than that of a two-level system, and both the excited and the target states are generally time dependent wave packets that vibrate on two different potentials. Thus, in order for a coherent transfer to occur over many vibrational periods, some form of a dynamical relation must be met: One option is that the two wave packets will vibrate "in unison," allowing a dynamic coherent transfer "as they move." Since the two wave packets have different vibrational periods, the duration of such a dynamic transfer is inherently limited by the vibrational frequency difference between the two potentials $\tau_{\mathrm{dyn}} < 1/(\nu_e - \nu_t)$. Prolonging the coherent transfer beyond τ_{dyn}, is only possible if the dynamics of the target state can be "frozen," such that it remains stationary over the entire transfer, i.e., have it as an eigenstate of the target potential. Thus, near threshold, where the transfer is slow, the oscillator tends to select a single target state, whereas far above threshold, where the transfer duration is shortened, dynamical transfer is allowed and the selectivity of the target state is reduced.

Eventually, the coherent transfer duration is limited by the available coherence time T_2. Consequently, to populate a single target state, it is necessary that T_2 be long enough to allow target state selectivity, i.e., $T_2 > 1/(\nu_e - \nu_t)$. This can explain the differences between Li_2, K_2, and Rb_2 in target selectivity: The coherence time in our simulation was fixed at $T_2 = 25$ ps. For the light Li_2, the vibrational frequencies (and their differences) are high, so the selectivity criterion is well met. K_2 is heavier, and therefore, the requirement is only marginally fulfilled, yet good selectivity can be obtained near threshold. Rb_2, on the other hand, is too heavy and falls short of this criterion. If the coherence time in the experiment were longer, K_2 and Rb_2 could also show high selectivity, in addition to a reduced threshold.

To calculate the threshold, it is now necessary to estimate the homogeneous coherence time T_2 in the vapor cell, dictated by the collisional pressure broadening, and the available density for coherent gain, affected by the inhomogeneous distribution of rotational states. Since the pressure broadening for collisions of the molecules with the surrounding atoms (and buffer gas, if added) is of order 100 MHz/Torr, $T_2 \geq 100$ ps is easily achievable at atomic pressures up to 10 Torr. For inhomogeneous broadening, the major limitation is due to rotations, which are thermally populated up to $J \approx 100$. The optical emission frequency of each J state is slightly shifted due to the difference in rotational constants between the ground and excited potentials, effectively dividing the molecular medium into independent coherent clusters (J states), which experience gain at slightly different frequencies. Near threshold, only the most populated clusters can oscillate, reducing the density available for gain to 1.5%–5% of the total density. With these considerations, the threshold for K_2 medium in a cavity with 1% loss is estimated to require molecular density of 10^{13-14} cm^{-3} in a cell length of 5–10 cm,

pumped by ~500 mW at 50 MHz repetition rate (see Supplemental Material [21] for detailed decoherence considerations and threshold estimation).

The selective and efficient dumping to a single state is important since it enables unique reconstruction of the excited wave-packet dynamics from the emitted field. Specifically, spectral analysis of the emitted field fully reflects the vibrational structure of the excited potential (including phase), as detailed in the (see Supplemental Material [21]. We do not view the Raman oscillator as a new method for efficiently transferring population between ground levels, since it is rather complicated, and since other well established, robust, and efficient methods exist for population transfer between ground states, such as stimulated Raman adiabatic passage [46].

To conclude, a coherent Raman oscillator that amplifies emission from a coherently excited wave packet, appears within experimental reach. If realized, this oscillator can open a window to explore molecular coherent dynamics by amplifying the emitted signal per molecule by several orders of magnitude. The unique effects of mode competition between different coherent transfer possibilities in such an oscillator are of great interest.

This research was supported by the Israel Science Foundation (Grants No. 807/09 and No. 46/14).

*jigal2@gmail.com
†avi.peer@biu.ac.il

[1] G. Herzberg, *Molecular Spectra and Molecular Structure: Spectra of Diatomic Molecules*, 2nd ed. (Krieger, Malabar, FL, 1989), Vol. 1.
[2] P. Atkins and R. Friedman, *Molecular Quantum Mechanics* (Oxford University Press, Oxford, 2011).
[3] H. Katsuki, H. Chiba, B. Girard, C. Meier, and K. Ohmori, Science **311**, 1589 (2006).
[4] H. Katsuki, H. Chiba, C. Meier, B. Girard, and K. Ohmori, Phys. Rev. Lett. **102**, 103602 (2009).
[5] J. A. Yeazell and C. R. Stroud, Phys. Rev. A **43**, 5153 (1991).
[6] I. A. Walmsley and L. Waxer, J. Phys. B **31**, 1825 (1998).
[7] C. Leichtle, W. P. Schleich, I. S. Averbukh, and M. Shapiro, Phys. Rev. Lett. **80**, 1418 (1998).
[8] A. Monmayrant, B. Chatel, and B. Girard, Phys. Rev. Lett. **96**, 103002 (2006).
[9] T. C. Weinacht, J. Ahn, and P. H. Bucksbaum, Nature (London) **397**, 233 (1999).
[10] I. Walmsley, T. Dunn, and J. Sweetser, in *Coherence and Quantum Optics VII*, edited by J. Eberly, L. Mandel, and E. Wolf (Springer, New York, 1995), pp. 73–82.
[11] A. Pe'er, E. A. Shapiro, M. C. Stowe, M. Shapiro, and J. Ye, Phys. Rev. Lett. **98**, 113004 (2007).
[12] E. A. Shapiro, A. Pe'er, J. Ye, and M. Shapiro, Phys. Rev. Lett. **101**, 023601 (2008).
[13] M. C. Stowe, M. J. Thorpe, A. Pe'er, J. Ye, J. E. Stalnaker, V. Gerginov, and S. A. Diddams, in *Advances In Atomic, Molecular, and Optical Physics*, edited by P. R. B. Ennio Arimondo and C. C. Lin (Academic Press, 2008), Vol. 55, pp. 1–60.
[14] L. A. Nafie, J. Raman Spectrosc. **43**, 1845 (2012).
[15] J.-X. Cheng and X. S. Xie, *Coherent Raman Scattering Microscopy*, Series in Cellular and Clinical Imaging (CRC Press, 2012).
[16] C. W. Freudiger, W. Min, G. R. Holtom, B. Xu, M. Dantus, and S. XieX, Nat. Photonics **5**, 103 (2011).
[17] B. G. Saar, C. W. Freudiger, J. Reichman, C. M. Stanley, G. R. Holtom, and X. S. Xie, Science **330**, 1368 (2010).
[18] J. P. Pezacki, J. A. Blake, D. C. Danielson, D. C. Kennedy, R. K. Lyn, and R. Singaravelu, Nat. Chem. Biol. **7**, 137 (2011).
[19] A. Volkmer, L. D. Book, and X. S. Xie, Appl. Phys. Lett. **80**, 1505 (2002).
[20] N. Dudovich, D. Oron, and Y. Silberberg, Nature (London) **418**, 512 (2002).
[21] See Supplemental Material at http://link.aps.org/supplemental/10.1103/PhysRevLett.116.073603 for expanded description of the simulation techniques, decoherence estimations, and detailed analysis of the results, which includes Refs. [22–32].
[22] M. Born and E. Wolf, *Principles of Optics: Electromagnetic Theory of Propagation, Interference and Diffraction of Light*, 7th Ed. (Cambridge University Press, Cambridge, England, 1999).
[23] J. D. Jackson, *Classical Electrodynamics*, 3rd ed. (Wiley, New York, 1999).
[24] A. E. Siegman, *Lasers* (University Science Books, Sausalito, CA, 1986).
[25] *Laser Physics and Applications*, edited by G. Herziger, H. Weber, and R. Poprawe (Springer, New York, 2007), Vol. 1.
[26] M. Lapp and L. P. Harris, J. Quant. Spectrosc. Radiat. Transfer **6**, 169 (1966).
[27] C. B. Alcock, V. P. Itkin, and M. K. Horrigan, Can. Metall. Q. **23**, 309 (1984).
[28] A. F. J. van Raan, J. E. M. Haverkort, B. L. Mehta, and J. Korving, J. Phys. B **15**, L669 (1982).
[29] M. P. Auzin'sh, I. Y. Pirags, R. S. Ferber, and O. A. Shmit, Sov. JETP Lett. **31**, 554 (1980).
[30] P. Rosenberg, Phys. Rev. **55**, 1267 (1939).
[31] K. Lulla, H. H. Brown, and B. Bederson, Phys. Rev. **136**, A1233 (1964).
[32] G. A. Pitz, A. J. Sandoval, N. D. Zameroski, W. L. Klennert, and D. A. Hostutler, J. Quant. Spectrosc. Radiat. Transfer **113**, 387 (2012).
[33] P. Brumer and M. Shapiro, *Principles of the Quantum Control of Molecular Processes*, 2nd ed. (Wiley-Interscience, New York, 2011).
[34] D. J. Tannor and S. A. Rice, J. Chem. Phys. **83**, 5013 (1985).
[35] M. Shapiro and P. Brumer, J. Chem. Phys. **84**, 4103 (1986).
[36] M. Nixon, O. Katz, E. Small, Y. Bromberg, A. A. Friesem, Y. Silberberg, and N. Davidson, Nat. Photonics **7**, 919 (2013).
[37] V. Kimberg and N. Rohringer, J. Phys. Conf. Ser. **488**, 032019 (2014).
[38] V. Kimberg and N. Rohringer, Phys. Rev. Lett. **110**, 043901 (2013).
[39] I. Coddington, W. C. Swann, and N. R. Newbury, Phys. Rev. Lett. **100**, 013902 (2008).

[40] I. Coddington, W. C. Swann, and N. R. Newbury, Opt. Lett. **35**, 1395 (2010).
[41] B. M. Garraway and K. A. Suominen, Rep. Prog. Phys. **58**, 365 (1995).
[42] S. Magnier and P. Millié, Phys. Rev. A **54**, 204 (1996).
[43] P. Jasik and J. Sienkiewicz, Chem. Phys. **323**, 563 (2006).
[44] S. J. Park, S. W. Suh, Y. S. Lee, and G.-H. Jeung, J. Mol. Spectrosc. **207**, 129 (2001).
[45] M. Gehm, Properties of ^{6}Li, North Carolina State University Technical Report (2003), http://www.physics.ncsu.edu/jet/techdocs/pdf/PropertiesOfLi.pdf.
[46] K. Bergmann, H. Theuer, and B. W. Shore, Rev. Mod. Phys. **70**, 1003 (1998).